Fault detection of wind turbine gearbox using thermal network modelling and SCADA data

B. Corley, J. Carroll, A. McDonald

Wind Energy & Control Centre, University of Strathclyde, Glasgow, UK

becky.corley@strath.ac.uk

Abstract. This work uses a detailed understanding of the physics inside a wind turbine gearbox and SCADA temperature data as an alternative to data-driven techniques for fault detection. Thermal modelling based on the principles of heat transfer theory is used with the aim of understanding the thermal behaviour of a 'healthy' gearbox and use it to detect abnormal gearbox operating conditions. Data for turbines, 'healthy' and one month to fail, are analysed for two different failure modes to see if a fault can be detected in advance with the aim to improve physical understanding of wind turbine gearbox operation and condition monitoring techniques.

1. Introduction

The European Union has set a target for 2030 of at least 32% of energy from renewable sources [1] to meet its emissions reduction commitments under the Paris Agreement, to combat climate change. Operation and Maintenance (O&M) contributes up to 25% of the total levelised cost of wind energy, for onshore and up to 40% for offshore [2]. The wind turbine gearbox is notorious for contributing to this expense as failure incurs high costs for repair in addition to lost revenue from high downtime per failure [3]. A predictive maintenance strategy optimises asset life and resources to minimise O&M costs. To implement predictive maintenance, the condition of components must be regularly monitored. Condition monitoring refers to processes that enable early detection of faults, failures and wear of machinery before they reach a catastrophic or secondary-damage stage. It can also extend asset life, enable better maintenance planning and logistics, and can reduce routine maintenance [4], with the intention of minimising downtime, and O&M costs while maximising production [5].

In this work the authors propose using a detailed understanding of the gearbox physics to model gearbox thermal behaviour, so that failures can be identified, and thresholds can be set for anomalous gearbox temperature behaviour. This is especially useful when historical operational data is unavailable or when data is to be added to data driven anomaly detection techniques at a later stage, through incremental learning. Thermal modelling based on the principles of heat transfer theory is used to develop this understanding; exploiting temperature measurements to understand a 'healthy' gearbox, and then use it to detect abnormal gearbox operating conditions. This is based on the theory that gearboxes generate power losses in the form of heat. Modern wind turbines (which use gearboxes) measure the gearbox temperature as a proxy of gearbox health, but internal and external environment and machine conditions can influence temperature measurements, so by analysing the evolution of temperature, it is important to note if the increased temperature is from a fault or from higher load.

2. Nomenclature

Q	Heat flow (W)	h	Heat transfer coefficient $(W\ m^{-2}\ K^{-1})$
T	Temperature (K)	k	Thermal conductivity $(W\ m^{-1}\ K^{-1})$
R	Thermal resistance $(K\ W^{-1})$	HS	High Speed
C	Thermal conductance $(W\ K^{-1})$	IMS	Intermediate Speed
A	Area (m^2)	LS	Low Speed
L	Length (m)		

3. Existing condition monitoring and fault detection methods

Current state-of-the-art fault detection research uses data science techniques applied to wind turbine data. This takes the form of SCADA (Supervisory Control and Data Acquisition) data and additional condition monitoring systems (CMS) data which vary depending on the turbine type, size and operator. A range of techniques can be used for the CMS: acoustic measurement, electrical effect monitoring, power quality, temperature, oil debris monitoring and vibration analysis. The nature of these variables differ, therefore there are a range of ways in which the data can be analysed. These techniques and applications will briefly be explored.

3.1. Vibration

Vibration as a fault indicator has received a lot of attention in recent research. Accelerometers measure vibration signals and it is known that characteristics of a "healthy" vibration can be demonstrated, so in theory faults in gearbox components would result in changes to vibration data in the frequency or time-frequency domains [6]. A number of processing methods have been applied successfully such as Envelope Analysis, Wavelet-Transform, and Artificial Neural Networks to name a few. However, this analysis requires advanced signal processing as the data is noisy. Most vibration based fault detection is focused on high speed (HS) and intermediate speed (IMS) stages, as detecting faults in low speed (LS) stage is difficult due to weak fault signals [7]. Vibration analysis requires expensive sensory systems and maintenance and repair of these is an added cost.

3.2. Electrical signal analysis

Electrical signal analysis has the potential to reduce wind turbine operation cost by reducing the number of sensors, and therefore the need for maintenance and repair [6], as current and voltage signals are already monitored for operation. It has been found that vibrations inside the mechanical components appear in the electrical signatures of the wind turbine generator [6] [8]. Fault detection uses similar approaches to vibration analysis, such as Wavelet Transform, Fourier Transform, and Time Synchronous Averaging [6]. Researchers in [9] used current signature with vibration data to improve detection and diagnosis accuracy.

3.3. Oil analysis

Oil sample analysis takes a sample from the operational gearbox and investigates the oil chemical properties, viscosity, particle count and debris analysis. Oil monitoring can detect gear and bearing failure as damaged gearboxes have much higher debris generation rates than healthy gearboxes [10]. Lubricant parameters can be indicators for lubricant degradation, which would lead to further failures. Oil sample analysis is usually carried out offline, which can incur costs for access, and may detect faults too late.

3.4. SCADA data

All turbines use SCADA data of varying quality to relate wind turbine operating and environmental conditions: wind speed, temperature and power, with the condition of the system [11][12]. Using temperature data for fault detection can be successful [13][14][15] as it does not require complex signal processing. However, accurate fault detection and reliable prognosis in wind turbine gearboxes remain

challenging due to the inherent complexities in their mechanical systems and operation conditions. As a result, SCADA data analysis has become more complex, as an increasing amount of data is collected.

Techniques for data analysis can largely be grouped into: trending, clustering, normal behaviour modelling (NBM) and damage modelling. Trending is an arguably less complex method of analysis, but as a result it tends to be case specific requiring manual interpretation or, if used online, generates frequent false alarms [16]. Clustering techniques can be effective with enough data, but can also be difficult to interpret. NBM has become a popular approach to data analysis whereby a model for the normal behaviour is established using training data, and the difference between predicted and actual values of the parameters is then calculated. There are a number of techniques that can be applied to NBM, a prevalent method being neural networks, which has proved a successful means of detecting anomalies [17][18][19].

Finally, damage modelling is an alternative to the "black box" approach of the methods discussed previously, where physical processes relating to failure are modelled. Few studies have used this approach successfully [20][21] and as a result application has yet to be established [16]. This research uses the damage modelling approach by understanding the physics of thermal behaviour in the gearbox.

4. Methodology

Thermal network modelling can estimate the heat losses generated within the gearbox, using available SCADA data and engineering drawings. The gearbox components are split into a number of lumped mass isothermal nodes, and an energy balance is applied to each node, assuming steady state conditions, shown in (1).

$$\sum Q_{in} + \sum Q_{out} = 0 \tag{1}$$

Where Q_{in} is any heat energy generated at the node, for example, from friction. Q_{out} is heat moving away from the node via heat transfer. Q is a function of temperature difference (ΔT) and thermal resistance between two nodes, as shown in (2). Thermal resistance R_{a-b} is characterised by the type of heat transfer- conduction or convection, (3a) and (3b) respectively. Where A and L are related to component geometry, k and h are heat transfer properties.

$$Q_{a-b} = \frac{(T_a - T_b)}{R_{a-b}} \tag{2}$$

$$R_{conduction} = \frac{L}{A \times k} \qquad R_{convection} = \frac{1}{A \times h} \tag{3a, 3b}$$

A thermal network diagram for an example gearbox is shown in Figure 1, where gearbox components are connected by the thermal resistances (3a) and (3b). Carrying out an energy balance on each node results in a number of simultaneous equations as shown by (4a-4e), where C is the inverse of the calculated resistances.

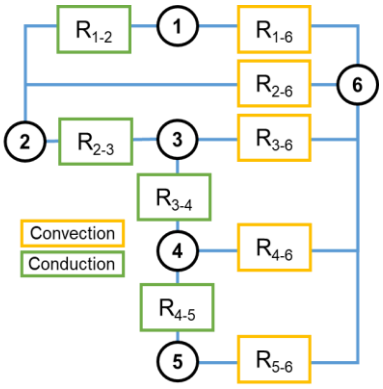

Figure 1: Thermal network model of gearbox for dataset 1

Node 1: $$\boldsymbol{Q_1 + T_6 C_{1-6} = T_1(C_{1-2} + C_{1-6}) - T_2 C_{1-2}} \quad (4a)$$

Node 2: $$Q_2 + T_6 C_{2-6} = -T_1 C_{1-2} + T_2(C_{1-2} + C_{2-3} + C_{2-4} + C_{2-6}) - T_3 C_{2-3} - T_4 C_{2-4} \quad (4b)$$

Node 3: $$Q_3 + T_6 C_{2-6} = -T_2 C_{2-3} + T_3(C_{2-3} + C_{3-4} + C_{3-6}) - T_4 C_{3-4} \quad (4c)$$

Node 4: $$Q_4 + T_6 C_{4-6} = -T_3 C_{3-4} + T_4(C_{3-4} + C_{2-4} + C_{4-5} + C_{4-6}) - T_2 C_{2-4} - T_5 C_{4-5} \quad (4d)$$

Node 5: $$Q_5 + T_6 C_{5-6} = -T_4 C_{4-5} + T_5(C_{4-5} + C_{5-6}) \quad (4e)$$

Node 6, the oil inlet, is treated as independent from the other nodes as its temperature is not affected by the temperature changes of the other nodes. This is because it is just after the oil has been through the heat exchanger to cool, and it is assumed that the auxiliary cooling system keeps the oil at a set temperature. These simultaneous equations can be rearranged into matrix form and solved, using the temperature SCADA data as demonstrated by (5).

$$\begin{bmatrix} T_1 \\ \vdots \\ T_n \end{bmatrix} \begin{bmatrix} (C_1 + C_2) & \cdots & -C_n \\ \vdots & \ddots & \vdots \\ -C_n & \cdots & (C_2 + C_n) \end{bmatrix} = \begin{bmatrix} Q_1 \\ \vdots \\ Q_n \end{bmatrix} \quad (5)$$

In this study, two datasets are used. Dataset 1 includes a number of turbines of the same type, that all share the same failure mode. Dataset 2 includes a number of turbines of the same type which differ from those of dataset 1. They share a common failure, different from dataset 1. This allows for different types of gearboxes to be modelled with different failure modes. All the gearboxes have a conventional set up for multi MW wind turbine, 3-stages, two planetary and one parallel. The temperature data available dictates the number and location of nodes to be used in the model, and therefore the heat transfer between nodes. Figure 2 shows the modelling process general to all gearbox applications.

Data one year to failure is considered healthy, and one month to failure (1M2F) is considered to have a fault which will lead to failure. As part of the data selection step, the power curves of the turbines are compared for healthy and 1M2F, to check for de-rating or other power curve deviations so that the same turbine can be compared for healthy and with fault.

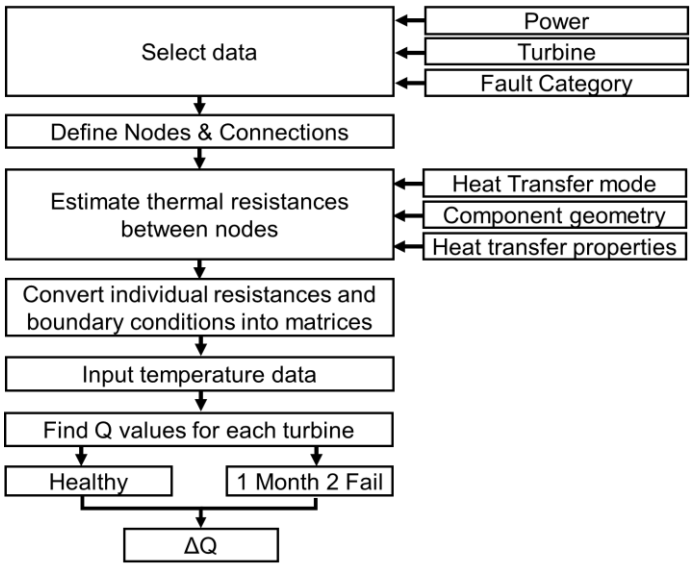

Figure 2: Methodology flowchart

5. Results

Temperature has historically been a used as a proxy for gearbox health. However, internal and external environment and machine conditions can influence temperature measurements, so by analysing the evolution of temperature, it is important to note whether the increased temperature is from a fault, or from higher load. This is why temperature differences due to faults are not always visible through graphing temperature alone. Figure 3 shows temperature data for a turbine with HS bearing failure, healthy and one month to fail. The temperature data has been binned into intervals of power and then the mean and standard deviation of each bin is plotted. The closeness of the lines and overlap of standard deviation bars show that the difference in temperature values are not consistently different enough to be relied upon for fault detection. This would result in faults being missed or false alarms.

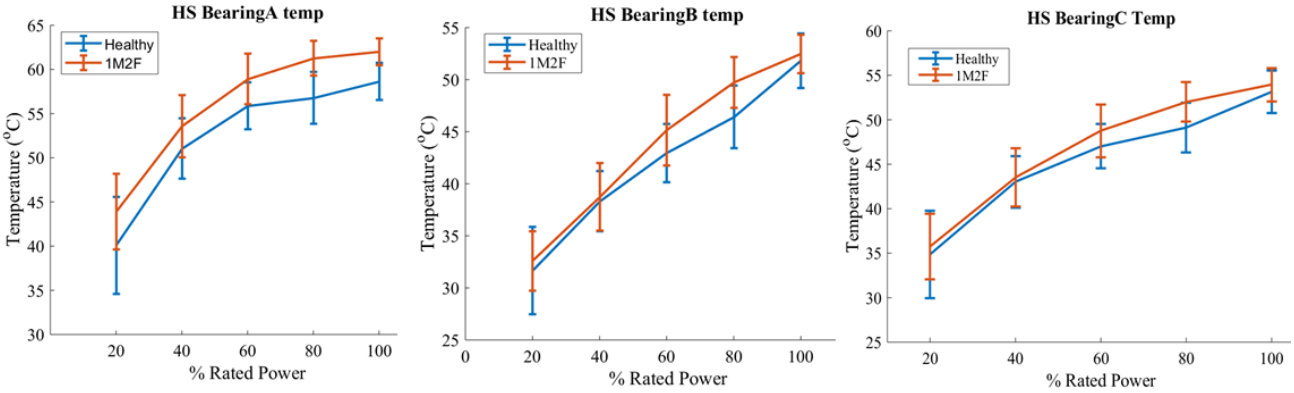

Figure 3:Temperature data for turbine with HS fault

5.1. Data set 1

Dataset 1 is a group of turbines of the same type that have a suffered a HS bearing fault. A thermal network diagram for an example gearbox is shown in Figure 1 and the node numbers corresponding to sensor location in Table 1 .

Sensor number	Location (node)
1	LS main bearing
2	IMS bearing (IMS)
3	HS bearing A (HSA)
4	HS bearing B (HSB)
5	HS bearing C (HSC)
6	Oil inlet

Table 1: Dataset 1 gearbox node labels

The calculated losses from a healthy turbine at rated power suggest a drive train efficiency of 90%, a value which is not unreasonable for a multi MW turbine. A difference in losses for a turbine with a HS bearing fault can be seen significantly at the HS bearing nodes. Figure 4 shows the mean and standard deviation of the losses from the same turbine healthy, and one month to failure, when at rated power, and there is a clear distinction.

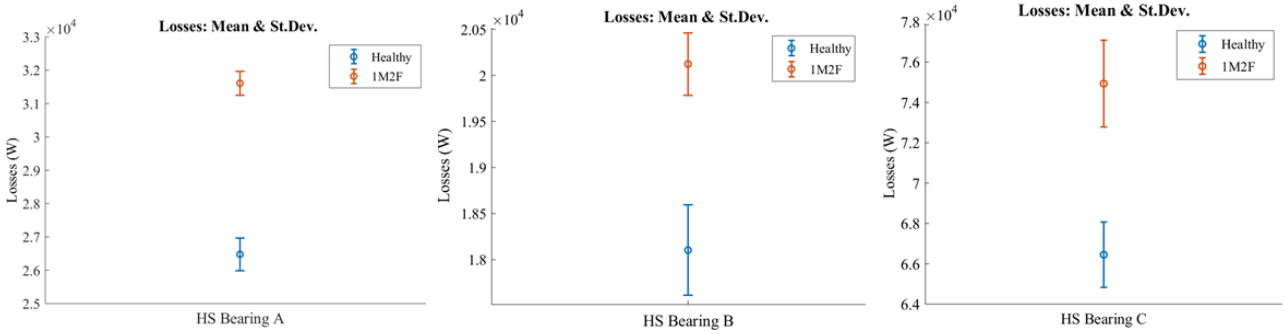

Figure 4: Losses at HS bearings

This method was applied to data from other turbines of the same type with a high-speed bearing fault. It should be noted that data cleaning was carried out and as a result not all turbine data was usable. From the remaining data, the results are shown in Table 2. The results are shown as the mean increase in heat losses (Q) between healthy and one month to fail as a percentage, with corresponding values of standard deviation (StD). T1 in Table 2 are the results from Figure 4 presented numerically. The results show a difference in losses between healthy and one month to fail, as shown in Table 2. For all turbines analysed, this did not apply at the LS node. The results are not listed as it gave negative losses. This is due to temperature at LS bearing being lower than oil inlet temperature. Further refinement of the model will be needed to rectify this.

Moreover, the results in table 2 show that, although this method in general shows an increase in heat losses one month to fail, when a level of uncertainty is applied in the form of standard deviation, the results are less convincing.

Q % increase		T1		T2		T3		T4		T5		T6	
		Mean	StD	Mean	StD	Mean	StD	Mean	StD	Mean	StD	Mean	StD
	HSA	20	2.6	4	5.0	0.9	3.8	6.0	2.3	0.8	3.8	0.53	2.5
	HSB	12	3.3	14	8.4	1.6	1.6	6.7	2.7	2.6	12.9	5.7	8.9
	HSC	13	4.2	10	5.1	0.66	3.4	5.8	2.2	2.6	8.6	3.8	5.3
	IMS	17	2.0	-7	11	1.0	2.8	4.6	4.1	0.55	7.5	2.8	9.1

Table 2: % increase in losses from HS bearing fault for turbines 1-6 from dataset 1

5.2. Dataset 2

For all turbines in dataset 1, the temperature sensors were located at the fault location. For dataset 2, all turbines have suffered with an IMS planetary bearing fault, but the gearbox configuration meant that the sensors were only located at the HS stage, not at the fault location, as is dataset 1. This will allow us to see if the method works when there are multiple heat transfer mechanisms in between the sensors and a fault.

The thermal network model of this gearbox configuration is shown in Figure 5, with Figure 6 and Table 3 showing the node locations.

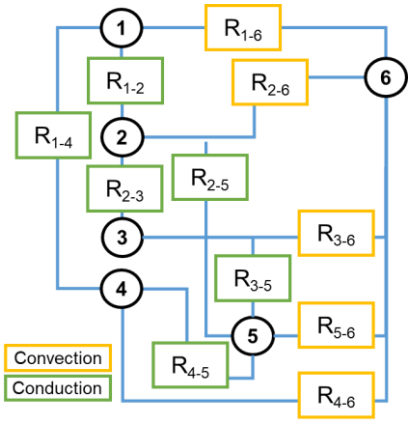

Figure 5: Thermal network model of gearbox for dataset 2

Sensor number	Location (node)
1	HS Rotor End (HSrtr)
2	HS Mid (HSmid)
3	HS Generator End (HSgen)
4	HS-lower speed Shaft Rotor End (Hlwrtr)
5	HS-lower speed Shaft Generator End (Hlwgen)
6	Oil inlet

Table 3: Dataset 2 gearbox node labels

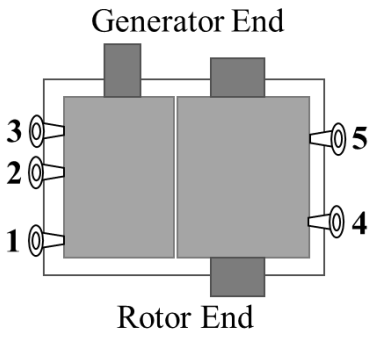

Figure 6: Schematic of gearbox HS end with sensor locations

Table 4 shows the difference in the losses between healthy and one month to a planetary bearing failure. As before with dataset 1, the change in losses varies in magnitude. The results are less consistent that dataset 1 but there are certain components that experience an increase in losses in many cases, namely “HS Gen” and “HS mid”.

	T1		T2		T3		T4		T5		T6		T7	
	Mean	StD	Mean	StD	Mean	StD	Mean	StD	Mean	StD	Mean	StD	Mean	StD
HSrtr	-5.4	2.0	-1.07	7.3	-1.89	4.1	9.5	3.0	-0.98	5.8	1.9	3.6	5.05	3.9
HSmid	34.5	2.0	1.2	2.4	1.2	2.2	6.9	2.4	12.7	4.1	1.3	4.5	6.44	4.6
HSgen	27.4	3.2	3.6	5.8	-0.2	5.4	12	4.8	9.4	6.3	-3.4	7.1	1.98	2.4
Hlwrtr	-22.0	2.4	-0.6	5.6	-3.01	3.5	11.1	4.4	0.44	5.1	-3.5	4.0	-3.24	7.0
Hlwgen	-19.9	1.5	-0.8	6.3	-0.78	5.5	8.4	4.7	0.02	5.4	-2.2	4.1	0.54	5.1

Table 4: % increase in losses from planetary bearing fault for turbines 1-7 from dataset 2

It should be noted that there are many factors that can influence the results at this stage. For example, the preprocessing of input data; temperature in relation to power and rotational speed. As a first iteration of this method, the results show potential, but also show that further work is needed to improve or disprove this damage modelling method as a potential failure detection tool.

6. Discussion

By applying SCADA temperature data to the thermal model, a change in heat losses can be seen to an extent. This change in losses at component level can provide an understanding of how a fault can affect the thermal behaviour of a gearbox. It has been found that when the fault is located close to the sensor, the thermal model shows the change more clearly. To increase confidence in the model, a weighting analysis is carried out using machine learning techniques, to see if the results from the physical model align with purely data-driven analysis.

6.1. Weighting analysis

Weighting analysis was undertaken to provide an insight into how the input variables affect how the turbines are classified in terms of healthy or one month to fail. For example, the results in Table 4 would suggest that "HS Gen" and "HS mid" are seeing the effects from the increase in losses at the planetary bearing fault.

To test this, dataset 2 was split into training and test data, and input into a two-class classifier model then a feature selection was carried out. Permutation feature importance (PFI) was the feature selection applied as it can capture how much influence each feature has on predictions from the model. In this case, to see which temperature sensors had the greatest effect on the classification – healthy or one month to fail.

There are a number of different data analysis techniques available that could be used. To determine which classifier would give the best results for the dataset, a preliminary analysis was carried out using Microsoft Azure Machine Learning Studio. Each turbine was tested individually for a range of two-class classifiers. The performance of the classifiers is measured in the form of accuracy and recall: accuracy being the fraction of correct predictions made for all inputs, and recall being the proportion of actual positives identified correctly out of all the inputs that should have been identified as positive. Recall is important when working with a class-imbalanced data set and when the cost of misclassification of the minor class is high. Table 5 summaries the performance of the classifiers, with the best performing highlighted.

		Neural network	**Support vector machine**	**Boosted decision tree**	**Random forest**	**Bayes point machine**
T1	Accuracy	1	1	1	1	0.97
	Recall	1	1	1	1	0.995
T3	Accuracy	0.735	0.557	0.876	0.869	0.569
	Recall	0.762	0.636	0.899	0.893	0.659
T4	Accuracy	0.619	0.564	0.809	0.787	0.564
	Recall	0.607	0.566	0.852	0.821	0.566
T6	Accuracy	0.756	0.687	0.881	0.866	0.684
	Recall	0.712	0.648	0.869	0.861	0.652
T7	Accuracy	0.906	0.789	0.973	0.975	0.772
	Recall	1	0.762	0.975	0.985	0.733
T8	Accuracy	0.755	0.547	0.859	0.854	0.587
	Recall	0.779	0.55	0.911	0.894	0.578
T10	Accuracy	0.785	0.743	0.946	0.941	0.641
	Recall	0.732	0.734	0.957	0.953	0.656

Table 5: Performance of Two-Class Classifiers

The two-class boosted decision tree classifier has the best results across most of the turbines, so this classifier was selected to apply PFI analysis. The PFI score given to each variable reflects the importance of the variable in the resulting classification. Figure 7 shows the importance of the temperature value for each sensor. The result are not perfectly clear, but it can be seen that "HSmid" has high scores for most of the turbines suggesting it is an important variable when determining if the turbine is healthy or one month to fail. This aligns with the results of the thermal modelling whereby 6/7 turbines showed additional losses at "HSmid" one month to failure. This has the potential to be important as it could provide insight as to how the losses propagate through the gearbox. Further exploration will be required.

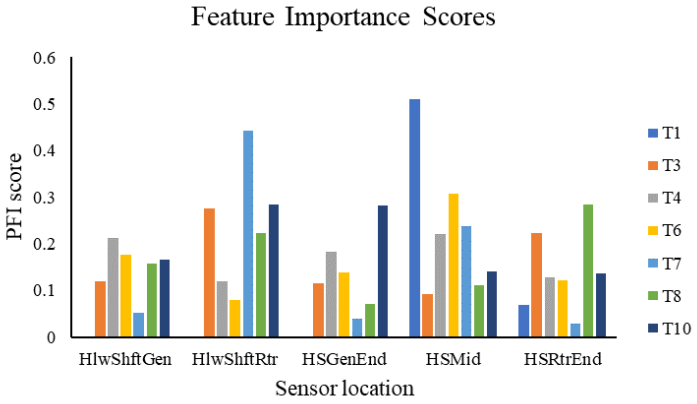

Figure 7: PFI scores for turbines in dataset 2

7. Further work

It should be noted that in this fairly simple thermal model, there are some thermal properties that have not been accounted for, thermal heat capacity being the most significant. Further research should determine the significance of ignoring its effects and refine the model if necessary.

In addition to refining the thermal model through revisiting assumptions, it is also important to quantify uncertainty of assumptions made in the model.

Finally, a more in-depth PFI analysis of the variables could provide further validation and allow refinement of the model. Next steps would be to optimize the classifier and carry out steps to ensure it does not overfit the data.

8. Conclusions

In this work thermal network modelling based on physical understanding of heat transfer combined with SCADA temperature data has shown that the differences between healthy and unhealthy gearboxes are clearer in the heat and power domain, than they are in the temperature domain. The modelling works best when the temperature sensor location corresponds to the fault location, but with further investigation and refinement, the model could detect faults at locations in the gearbox away from the sensors.

This theory has the potential to set condition monitoring threshold values for operational wind turbine gearboxes, by applying thermal modelling and gearbox power loss calculations [22] for a healthy gearbox. This would be applied to gearboxes of different configurations, without the need for historical operational data and failure history. By improving the accuracy of condition monitoring, the cost of wind turbine O&M can be reduced.

9. Acknowledgements

This work has been funded by the EPSRC, project reference number EP/L016680/1. The authors would like to acknowledge the help and guidance of Dr Sofia Koukoura in understanding machine learning techniques used in this paper.

10. References

[1] "Renewable energy directive | Energy." [Online]. Available: https://ec.europa.eu/energy/en/topics/renewable-energy/renewable-energy-directive/overview. [Accessed: 21-Nov-2019]
[2] Jantara V L and Papaelias M 2020 "Wind turbine gearboxes: Failures, surface treatments and condition monitoring," *Non-Destructive Testing and Condition Monitoring Techniques for Renewable Energy Industrial Assets* (Oxford: Butterworth-Heinemann) 69-90
[3] Carroll J, McDonald A, Feuchtwang J and D. McMillan 2014 "Drivetrain availability in offshore wind turbines," *European Wind Energy Association 2014 Annual Conference*
[4] Kim K, Parthasarathy G, Uluyol O, Foslien W, Sheng S and Fleming P 2011 "Use of SCADA data for failure detection in wind turbines," *2011 Energy Sustainability and Fuel Cell Conf.*
[5] de Azevedo H D M, Araújo A M, and Bouchonneau N 2016 "A review of wind turbine bearing condition monitoring: State of the art and challenges," *Renew. Sustain. Energy Rev.* **56** 368–379
[6] Salameh J P, Cauet S, Etien E, Sakout A, and Rambault L 2018 "Gearbox condition monitoring in wind turbines: A review," *Mech. Syst. and Signal Process.* **111** 251–264
[7] Liu Z and Zhang L 2020 "A review of failure modes, condition monitoring and fault diagnosis methods for large-scale wind turbine bearings," *Measurement*
[8] Cheng F, Qu L, Qiao W, Wei C, and Hao L 2019 "Fault Diagnosis of wind turbine gearboxes based on DFIG stator current envelope analysis," *IEEE Trans. Sustain. Energy* **10** 1044–53
[9] Artigao E *et al.* 2018 "Current signature and vibration analyses to diagnose an in-service wind turbine drive train," *Energies* **11** 960
[10] Sheng S 2016 "Monitoring of wind wurbine gearbox condition through oil and wear debris analysis: A full-scale testing perspective," *Tribol. Trans.* **59** 149–162
[11] Nie M, and Wang L 2013 "Review of condition monitoring and fault diagnosis technologies for wind turbine gearbox," *Procedia CIRP* **11** 287–290
[12] Zaher A,McArthur S D J, Infield D G and Patel Y 2009 "Online wind turbine fault detection through automated SCADA data analysis," *Wind Energy* **12** 574–593
[13] Feng Y, Qiu Y, Crabtree C J, Long H, and Tavner P J 2011 "Use of SCADA and CMS signals for failure detection and diagnosis of a wind turbine gearbox," *EWEC 2011* 17–19.
[14] Astolfi D, Castellani F and Terzi L 2014 "Fault prevention and diagnosis through SCADA temperature data analysis of an onshore wind farm," *Diagnostyka* **15**
[15] Touret T, Changenet C, Ville F, Lalmi M and Becquerelle S 2018 "On the use of temperature for online condition monitoring of geared systems – A review," *Mech. Syst. Signal Process.* **101** 197–210
[16] Tautz-Weinert J and Watson S J 2017 "Using SCADA data for wind turbine condition monitoring - A review," *IET Renewable Power Generation* **11** pp 382–394
[17] Bangalore P, Letzgus S, Karlsson D and Patriksson M 2017 "An artificial neural network-based condition monitoring method for wind turbines, with application to the monitoring of the gearbox," *Wind Energy* **20** 1421–38
[18] Schlechtingen M and Ferreira Santos I 2011 "Comparative analysis of neural network and regression based condition monitoring approaches for wind turbine fault detection," *Mech. Syst. Signal Process.* **25** pp 1849–75
[19] Zhang Z Y and Wang K S 2014 "Wind turbine fault detection based on SCADA data analysis using ANN," *Adv. Manuf.* **2** 70–78
[20] Qiu Y, Feng Y, Sun J, Zhang W, and Infield D 2016 "Applying thermophysics for wind turbine drivetrain fault diagnosis using SCADA data," *IET Renew. Power Gener.* **10** pp 661–668
[21] Gray C S and Watson S J 2009 "Physics of Failure approach to wind turbine condition based maintenance," *Wind Energy* **13** 395–405
[22] British Standard 2001 "BS ISO/TR 14179-2:2001 Gears - Thermal capacity - Part 2: Thermal load carrying capacity,"